

COMPARISON BETWEEN SOME DYNAMIC AND STATIC MODELS DESCRIBING THE PLASTIC ZONE

Alexandre Mikowski

Universidade Federal do Paraná, Dep. de Física, Cx. Postal 19044, Centro Politécnico, CEP 81531-990
Curitiba, PR
amikowski@bol.com.br

Carlos Eugênio Foerster and Francisco Carlos Serbena

Universidade Estadual de Ponta Grossa, Dep. de Física, Av. Carlos Cavalcanti, 4748, CEP 84.030-900,
Ponta Grossa, PR
carlofef@uepg.br and fserbena@uepg.br

Abstract. Several analytical models consider the dislocations that form the plastic zone around the crack tip as a continuous distribution of infinitesimal dislocations at static equilibrium due to a friction stress. Other models consider the dynamic evolution of the plastic zone with time and the description is based on computer simulations where the plastic zone is considered as formed by discrete dislocations not in equilibrium whose dynamics is described by a power relation between velocity, total stress and temperature. In this work, computer simulations are performed considering an infinite crack loaded under a fixed loading rate (Hirsch et al., 1989). The dislocations are emitted by a Frank-Read source positioned at a fixed distance ahead of the crack tip and in a plane that contains the crack front. From the simulations, the plastic zone size, the dislocation free zone, the total number and the distribution of dislocations, the elastic stress and the effective stress intensity factor are calculated. The results for mode I loading are compared with the static analytic model of (Chen et al, 1999). For mode III, the simulations are compared with the models of (Chang et al., 1981) and (Majumdar et al., 1983).

Keywords. crack, plastic zone, dislocations, analytical models

1. Introduction

The majority of crystalline solids fail by cleavage at low temperatures and by plastic deformation at high temperatures. In between these two regimes, a transition from brittle to ductile behavior is observed as the temperature increases. The transition is characterized by a gradual increase of fracture toughness over a region of 100 K or more. The bcc metals, some intermetallic alloys, MgO and other materials exhibit such transition (Roberts, 1997). In Si and sapphire single crystals, the transition is sharp, occurring over a temperature range less than 10 K⁽¹⁾. Several experiments of pre-cracked samples of several materials as Ge (Serbena et al., 1994), TiAl (Booth et al., 1997), NiAl (Serbena, 1995) and W (Gumbsch et al., 1998) showed the fracture toughness increases gradually with temperature and the brittle-ductile transition temperature depends on the applied strain rate. This increase is related with a higher dislocation mobility, resulting an increase in the plastic zone around the crack with the subsequent rise in crack tip shielding.

In this work, computer simulations of dislocations generated by a Frank-Read source positioned in front of the crack tip under different loading modes are described. The main purpose is the comparison of the dynamic model according to Hirsch, Roberts & Samuels – HRS (Hirsch et al., 1989) with analytical models where the plastic zone is at equilibrium under the action of a friction stress according to the models of Chen & Kitaoka – CK (Chen et al., 1999, Chang & Ohr – CO (Chang et al., 1981) and Majumdar & Burns - MB (Majumdar et al., 1983).

2. The numerical simulations of the Hirsch et al model for different modes

The plastic zone is assumed to be located in a single slip plane which intercepts the whole crack front as shown in figure 1. The angle between the slip plane and the crack plane is θ . For mode I, θ is 90° and for modes II and III, θ is equal to 0°. A Frank-Read source is positioned along the slip plane at a fixed distance x_c equals to 10b ahead of the crack front for the simulations, where b is the dislocation Burgers vector.

The source emits a single edge (modes I and II) or a screw (mode III) dislocation every time the stress at the source is positive. The shear stress σ_{xy} at an edge dislocation positioned at a distance y_i emitted in mode I is (Hirsch et al., 1989):

$$\sigma_{xy} = \frac{K_I}{4(\pi y_i)^{1/2}} - \frac{\mu b}{4\pi(1-\nu)y_i} + \frac{\mu b}{4\pi(1-\nu)} \sum_{j \neq i} \left\{ \left(\frac{y_j}{y_i} \right)^{1/2} \frac{1}{(y_i - y_j)} + \frac{8y_i y_j}{(y_i + y_j)^3 (y_i - y_j)} \right\}, \quad (1)$$

where y_j is the position of the j^{th} edge dislocation, K_I is the mode I applied stress intensity factor, μ is shear modulus equals to 50 GPa, b is the Burgers vector equals to 4 \AA and ν is the Poisson coefficient assumed to be 0.3. For mode II, the shear stress σ_{xy} at any edge dislocation is given by (Hirsch et al., 1989):

$$\sigma_{xy} = \frac{K_{II}}{(2\pi x_i)^{1/2}} - \frac{\mu b}{4\pi(1-\nu)x_i} + \frac{\mu b}{2\pi(1-\nu)} \sum_{j \neq i} \left(\frac{x_j}{x_i} \right)^{1/2} \frac{1}{(x_i - x_j)}, \quad (2)$$

where x_j is the position of the j^{th} dislocation, K_{II} is the mode II applied stress intensity factor. For mode III, the stress σ_{xz} acting at a screw dislocation is (Hirsch et al., 1989):

$$\sigma_{xz} = \frac{K_{III}}{(2\pi x_i)^{1/2}} - \frac{\mu b}{4\pi x_i} + \frac{\mu b}{2\pi} \sum_{j \neq i} \left(\frac{x_j}{x_i} \right)^{1/2} \frac{1}{(x_i - x_j)}, \quad (3)$$

where K_{III} is the mode III applied stress intensity factor.

Simulations were also performed according to the analytical model for a mode I crack as proposed by Chen & Kitaoka (Chen et al., 1999). In their model, the dislocation interaction term is simpler than the one used by the HRS model shown in equation (1). In the CK model, the shear stress σ_{xy} at any edge dislocation positioned at y_i is:

$$\sigma_{xy} = \frac{K_I}{4(\pi y_i)^{1/2}} - \frac{\mu b}{4\pi(1-\nu)y_i} + \frac{\mu b}{2\pi(1-\nu)} \sum_{j \neq i} \frac{1}{(y_i - y_j)}. \quad (4)$$

In the equations (1-4), the first term refers to the crack tip stress field under the remote stress, the second is the image term and the third is the dislocation-dislocation interaction term in the presence of the crack. The dislocation mobility is described by an empirical relation in an Arrhenius form of $v = A\sigma^m \exp(-U/kT)$, where m is the stress exponent equals to 1, A is a constant equals to $1.05 \times 10^{-5} \text{ m.s}^{-1}.\text{Pa}^{-1}$, T is the temperature assumed to be 473 K, U is the activation energy for dislocation mobility equals to 1 eV, σ is the total stress and k is the Boltzmann constant.

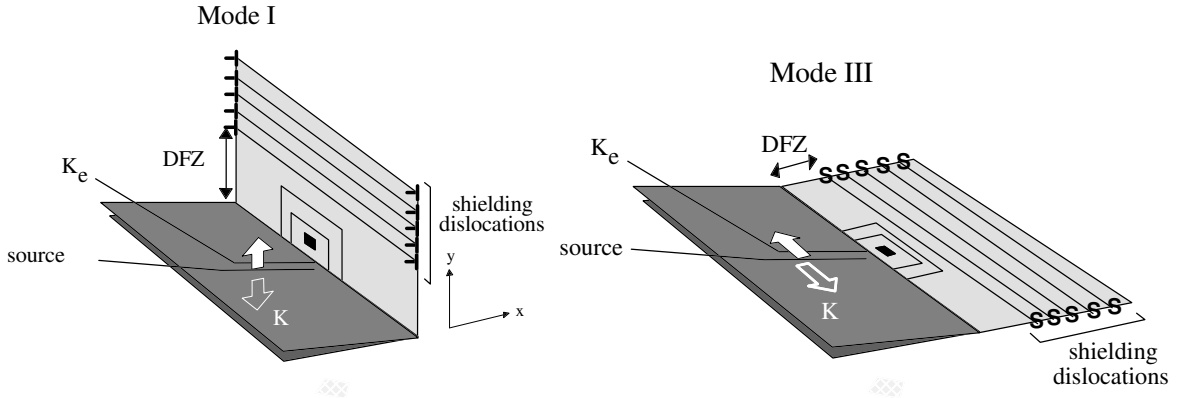


Figure 1. Plastic zones for modes I and III.

The simulations were performed at a constant applied stress intensity factor rate for the corresponding mode. The value chosen was $\dot{K} = 1,0 \times 10^{-3} \text{ MPa.m}^{1/2}.\text{s}^{-1}$, which is the applied \dot{K} used in experiments reported in Serbena et al. (1994). At each time interval δt used in the program, the stress at the source is examined to verify if a new dislocation can be nucleated. If the stress is positive, a dislocation is generated at the source, the stress at each dislocation is calculated and they move at a distance equal to $\delta t v_i$. The applied stress intensity factor is increased by $\delta t \dot{K}$ at each cycle and the effective stress intensity factor K_e at the crack tip is calculated as (Hirsch et al., 1989):

$$K_e = K + K_S, \quad (5)$$

where K_S is the shielding effect due to crack-dislocation interaction. As the time and the applied K increase with time, K_e also increases, due to the increasing number of dislocations emitted by the source and the increase in plastic zone size. The stress intensity at fracture K_F can be calculated if the criterion for fracture is taken as when $K_e = K_{IC}$.

The time interval δt was calculated at each cycle in a manner that the dislocations in the array would move at most a 1/3rd of the distance to the adjacent's dislocation old position. Simulations were also performed for smaller fractions of the distance (smaller δt) and the obtained results were the same.

As the computer time increases as $n!$, an algorithm which "bundled" the dislocations into superdislocations was used to reduce computer time requirements (Hirsch et al., 1989). The dislocations were grouped into superdislocations with Burgers vector Nb , where N is the number of "bundled" dislocations. The arrangement is such the distribution of (super)dislocations in the plastic zone is 1.1.1.3.3.3.9.9.9.27.27.27...27.27.27.9.9.9.3.3.1.1.1 in respect to their Burgers vectors.

3. Description of the static analytical models

3.1. Static analytic model for mode I by Chen & Kitaoka

The problem of a infinite crack loaded under mode I, with a simplified description of the dislocation-dislocation interaction term around the crack tip and with the inclusion of a DFZ was treated by *Chen & Kitaoka* (Chen et al., 1999) and *Chen & Takezono* (Chen et al., 1995). The dislocations are emitted on an inclined plane and form a plastic zone of size a , leaving behind a dislocation free-zone of size e . The dislocations are at rest under the action of a friction stress. Once dislocations are emitted, they interact elastically with the crack, reducing the local effective stress intensity factor at the crack tip. The problem is treated under plane strain condition, and the equilibrium equation for each dislocation is composed of 4 terms: the crack tip stress field, the dislocation-dislocation interaction, the image stress and the friction stress. The distribution is assumed to be made of dislocations with infinitesimal Burgers vector and is assumed to be continuous. The distribution $f(x)$ in the region $e < x < a$ satisfy the following equation of equilibrium (Chen et al., 1999):

$$\frac{\mu b}{2\pi(1-\nu)} \int_e^a \frac{f(x)}{r-x} dx = \sigma(r), \quad (6)$$

where $\sigma(r)$ is the total stress and is given by:

$$\sigma(r) = \sigma_f - \frac{K_I \sin \theta \cos \frac{1}{2}\theta}{2\sqrt{2\pi r}}, \quad (7)$$

where σ_f is the friction stress, r and θ are the polar coordinates. In this model, the image term is neglected. Equation (6) is a singular integral equation, where $f(r)$ is limited between e and a . The solution is (Chen et al., 1999):

$$f(r) = \frac{2(1-\nu)\sigma_f}{\mu b} \sqrt{\frac{a}{r}} \left[E\left(\phi, k\right) - \frac{E\left(\frac{\pi}{2}, k\right)}{F\left(\frac{\pi}{2}, k\right)} F\left(\phi, k\right) \right], \quad (8)$$

where $F\left(\frac{\pi}{2}, k\right)$ and $E\left(\frac{\pi}{2}, k\right)$ are the complete elliptical integrals of first and second kind, $F(\phi, k)$ and $E(\phi, k)$ are the incomplete elliptical integrals of first and second kind respectively, $\phi = \arcsen \sqrt{\frac{(a-x)}{(a-e)}}$ is the argument of the

elliptical integrals, $k = \sqrt{1 - \frac{e}{a}}$ is the modulus, e is the size of the DFZ and a is the plastic zone size. The condition for DFZ is (Chen et al., 1999):

$$\pi\sigma_f - \frac{K_e \sin \theta \cos \frac{1}{2}\theta}{\sqrt{2\pi a}} \times F\left(\frac{\pi}{2}, k\right) = 0. \quad (9)$$

This expression establishes a relation between the local effective stress intensity factor K_e , the plastic zone size a and the DFZ size e . The total number of dislocations is given by integration of the distribution function in the interval $e < x < a$ and the result is (Chen et al., 1999):

$$n = \frac{2\pi a(1-\nu)\sigma_f}{\mu b} \left[\left(1 - \frac{k^2}{2}\right) - \frac{E\left(\frac{\pi}{2}, k\right)}{F\left(\frac{\pi}{2}, k\right)} \right]. \quad (10)$$

If it is assumed the plastic zone size is much bigger than the DFZ, $k \approx 1$, $\theta = \pi/2$, $F\left(\frac{\pi}{2}, k\right) \approx \ln\left(\frac{4}{\sqrt{\alpha_c}}\right)$ and $E\left(\frac{\pi}{2}, k\right) \approx 1$ (Byrd et al., 1954). After some algebraic manipulation, the final results are:

$$n = \frac{2\pi a(1-\nu)}{\mu b} \left[\frac{1}{2} - \frac{1}{\ln\left(4\sqrt{\frac{a}{e}}\right)} \right] \sigma_f, \quad (11)$$

$$K_e = 2\pi^{3/2} \sqrt{a} \cdot \frac{1}{\ln\left(4\sqrt{\frac{a}{e}}\right)} \sigma_f. \quad (12)$$

3.2. Static analytic model for modes II and III by Chang & Ohr

Chang & Ohr (Chang et al., 1981) elaborated an analytical model for a mode III loaded crack under a remote applied stress σ_a . Ahead of the crack, there is a continuous distribution $f(x)$ of screw dislocations under equilibrium of a friction stress. If the crack is under mode II loading, edge dislocations are emitted and the mathematical formulation differs by a constant factor.

The slip plane is assumed to be coplanar with the crack front. In this case, the following singular integral equation must be solved (Chang et al., 1981):

$$\frac{\mu b}{2\pi} \left(\int_{-a}^{-e} + \int_{-c}^c + \int_e^a \right) \frac{f(x')}{x-x'} dx' + \sigma_a = 0, \quad (13)$$

for $x < c$ and:

$$\frac{\mu b}{2\pi} \left(\int_{-a}^{-e} + \int_{-c}^c + \int_e^a \right) \frac{f(x')}{x-x'} dx' + \sigma_a = \sigma_f, \quad (14)$$

for $-a < x < -e$ and $e < x < a$ and x' is the variable of integration.

The equations (13) and (14) are solved by a method developed by *Muskhelishvili* (Muskhelishvili, 1953; Head et al, 1955) and the solution is (Chang et al., 1981):

$$f(x) = \frac{4\sigma_f}{\pi\mu b} F\left(\frac{\pi}{2}, m\right) \left\{ \frac{Q(m^2 - Q^2)^{1/2}}{(1 - Q^2)^{1/2}} - \left[E(D, m) - \frac{E\left(\frac{\pi}{2}, m\right) F(D, m)}{F\left(\frac{\pi}{2}, m\right)} \right] \right\}, \quad (15)$$

where $D = \text{sen}^{-1}\left(\frac{Q}{m}\right)$, $Q(x) = \sqrt{\frac{(a^2 - x^2)c^2}{(a^2 - c^2)x^2}}$, $m = Q(e)$ and c is the crack length.

The effective stress intensity factor K_e in this model is (Chang et al., 1981):

$$K_e = \frac{4}{\sqrt{\pi}} \sqrt{e} \sigma_f F\left(\frac{\pi}{2}, m\right), \quad (16)$$

In the limit $a \gg e$, the above expression is (Byrd et al., 1954):

$$K_e = \frac{4}{\sqrt{\pi}} \cdot \sqrt{e} \cdot \ln \left(4 \cdot \sqrt{\frac{a}{e}} \right) \sigma_f \quad (17)$$

3.3. Static analytic model for mode III by Majumdar & Burns

Majumdar & Burns (Majumdar et al., 1983) treated the case of a crack under mode III loading. Screws dislocations are emitted in a plane that contains the crack front. The plastic zone is considered as a continuous distribution of dislocations and equilibrium under a friction stress. The condition for equilibrium is (Majumdar et al., 1983):

$$\int_e^a \sqrt{\frac{x}{x-e}} \frac{1}{(x-e)} f(x) dx = \sqrt{\frac{2\pi}{x}} \frac{K_{III}}{\mu b} - \frac{2\pi\sigma_f}{\mu b} \quad (18)$$

where K_{III} is the applied stress intensity factor and $f(x)$ is the dislocations distribution. The left term refers to the dislocation-dislocation interaction, the first right term is crack tip stress field and the second term is related to the friction stress. The image term is neglected.

By using the method developed by *Muskhelishvili* (Muskhelishvili, 1953; Head et al, 1955), $f(x)$ is (Majumdar et al., 1983):

$$f(x) = \frac{4\sigma_f}{\pi\mu b} \left[F\left(\frac{\pi}{2}, k\right) E(\phi, k) - E\left(\frac{\pi}{2}, k\right) F(\phi, k) \right] \quad (19)$$

where $\phi = \sin^{-1}\left(\frac{1}{\alpha}\right)$, $\alpha = k\sqrt{\frac{x}{x-e}}$ and $k = \sqrt{1-\frac{e}{a}}$.

The shielding K_S of the crack is (Majumdar et al., 1983):

$$K_S = 2\sqrt{\frac{2}{\pi}} F\left(\frac{\pi}{2}, k\right) \left[\frac{1}{\sqrt{1-k^2}} \frac{E\left(\frac{\pi}{2}, k\right)}{F\left(\frac{\pi}{2}, k\right)} - 1 \right] \sigma_f \sqrt{e} \quad (20)$$

In the limit $a \gg e$ (Byrd et al., 1954):

$$K_e = \sqrt{\frac{8}{\pi}} \sqrt{e} \ln \left(\frac{4}{\sqrt{\alpha_c}} \right) \sigma_f \quad (21)$$

4. Results

4.1. Comparison between numerical simulations and static analytical model by Chen & Kitaoka

Figures 2 (a) and (b) show the number of dislocations and the effective stress intensity factor as a function of the stress along the plastic zone as predicted by the static analytical model of CK and as a function of the stress at the leading dislocation of the array for numerical simulations also performed according to this model. In this case, the simulations were performed for mode I loading in a similar manner as the numerical simulations for the HRS model described in section (2) and using equation (4) for the total stress.

The e , a and σ values generated by the simulation was substituted in equations (11) and (12) to obtain the curves of the static analytical model for comparison. There is good agreement between the predictions of equations (11) and (4) in figure 1 (a). In figure 2 (b), the static model predicts an increasing positive K_e , while the simulations predict negative values. This behavior is due to the great number of dislocations emitted during the simulation, causing a considerable shielding effect.

The comparison between the results predicted by the models HRS and CK obtained by numerical simulations are shown in figures 3. The DFZ predicted by the CK model is smaller than those predicted by the HRS model (figure 3 (a)), which causes a higher shielding as shown in figure 3 (b). As shown in figures 3 (c), (d) and (e), the stress at the leading dislocation, the number of dislocations and the plastic zone size predicted by the CK model are considerably higher than those predicted by the HRS model. The results show the crack is strongly shielded in the CK model due to a higher number of dislocations, a larger plastic zone and a smaller DFZ. The shape of the dislocation distribution is similar for both models as shown in figure 3 (f).

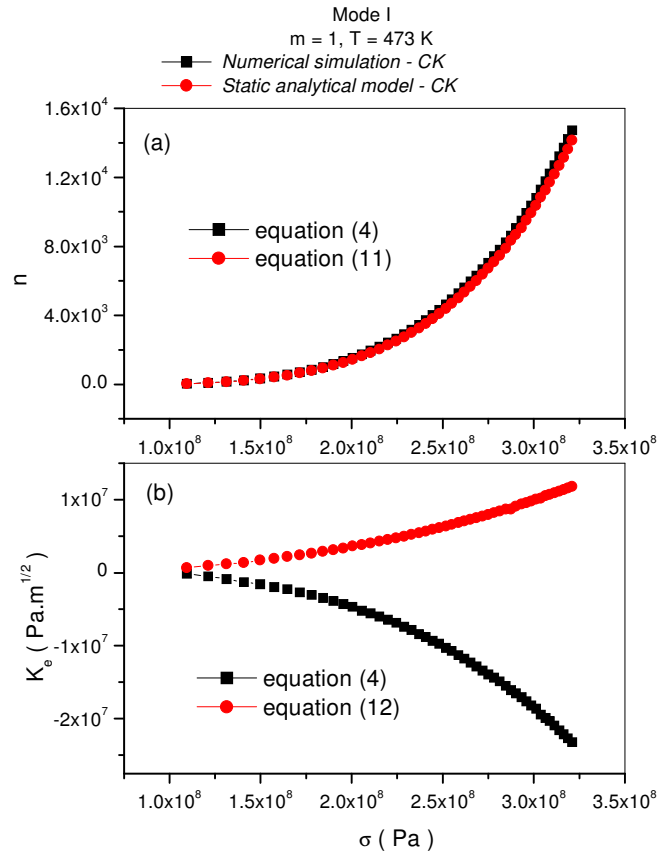


Figure 2. (a) Variation of number of dislocations and (b) effective stress intensity factor as a function of the stress along the plastic zone for the static analytical CK model and the stress at the leading dislocation of the array for numerical simulations according also to this model.

4.2. Comparison between numerical simulations and static analytical models by Chang & Ohr and by Majumdar & Burns

Numerical simulations according to the HRS model were performed and the results compared with the models CO and MB for mode III. The dislocation distribution of the HRS model agrees with that calculated by the MB model as shown in figure 4. The CO model predicts a lower distribution, indicating a lower number of dislocations in the plastic zone. This is also consistent when the effective stress intensity factor is calculated. Numerical simulations predicts a higher shielding than those calculated by the static models as shown in figure 5 (a). The least effective shielding is that predicted by the CO model. One reason for discrepancies between the simulations and the analytical models is that in all analytical models, the friction stress is assumed to be constant along the plastic zone. As can be seen in figure 5 (b), this is not the case when the total stress is calculated in the simulations. Although the stress can be considered fairly constant, it varies along the plastic zone.

5. Conclusions

In mode I, the number of dislocations in the plastic zone calculated by numerical simulations agrees with the results predicted by the model CK, but not the effective stress intensity factor. The simplified term for the dislocation-dislocation interaction term used in the CK model is not a good approximation, since the results predicted are not in accordance with those predicted by numerical simulations using the HRS model. This later model uses the correct term for dislocation-dislocation interaction in the presence of the crack.

In mode III loading, the dislocation distribution calculated by the model MB agrees with that calculated according to the HRS model. The shielding predicted by the HRS model differs from those calculated by the static models because the assumption of a constant friction stress along the plastic zone assumed in the analytical models does not hold for the numerical simulations.

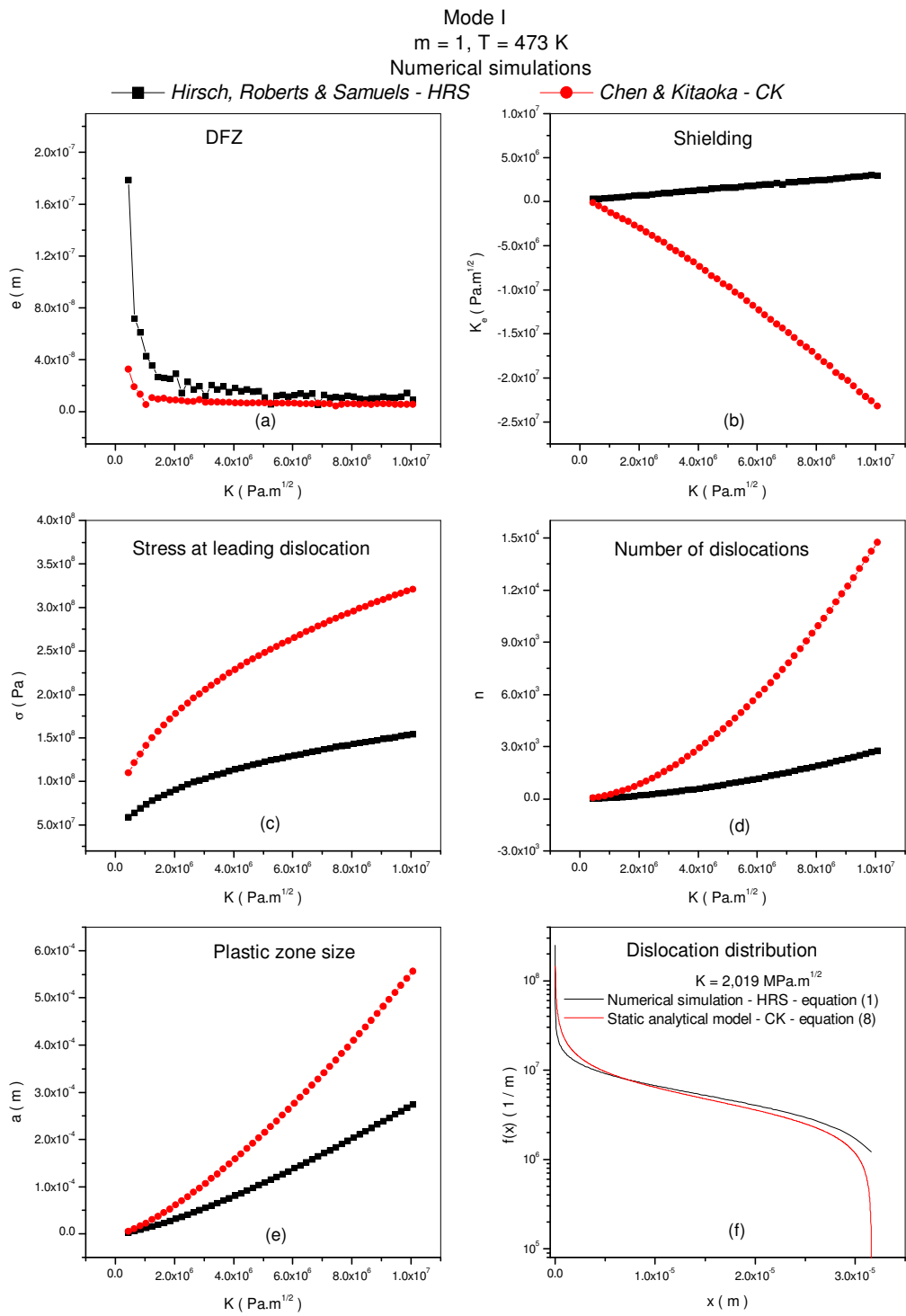


Figure 3. (a) DFZ, (b) effective stress intensity factor, (c) stress at the leading dislocation, (d) number of dislocations, (e) plastic zone size as a function of the applied K and (f) variation of dislocation density along the shear plane for an applied K of $2,019 \text{ MPa}\cdot\text{m}^{1/2}$.

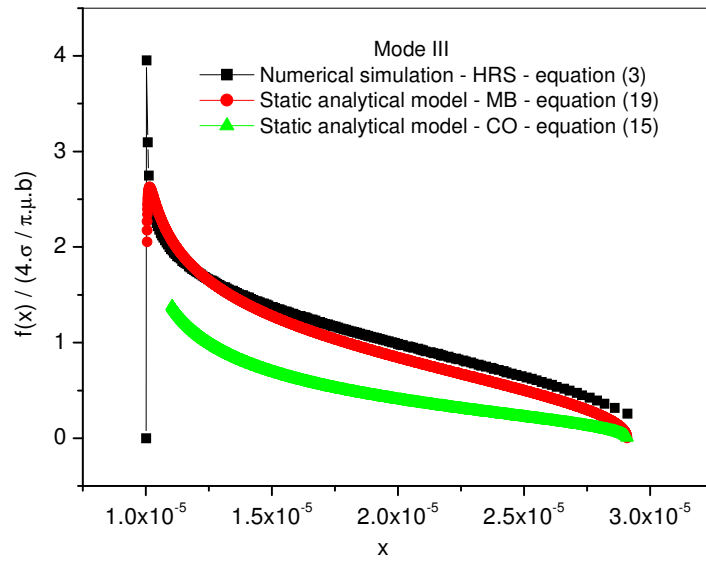


Figure 4. Normalized dislocation distributions along the plastic zone as calculated by the models HRS, MB and CO.

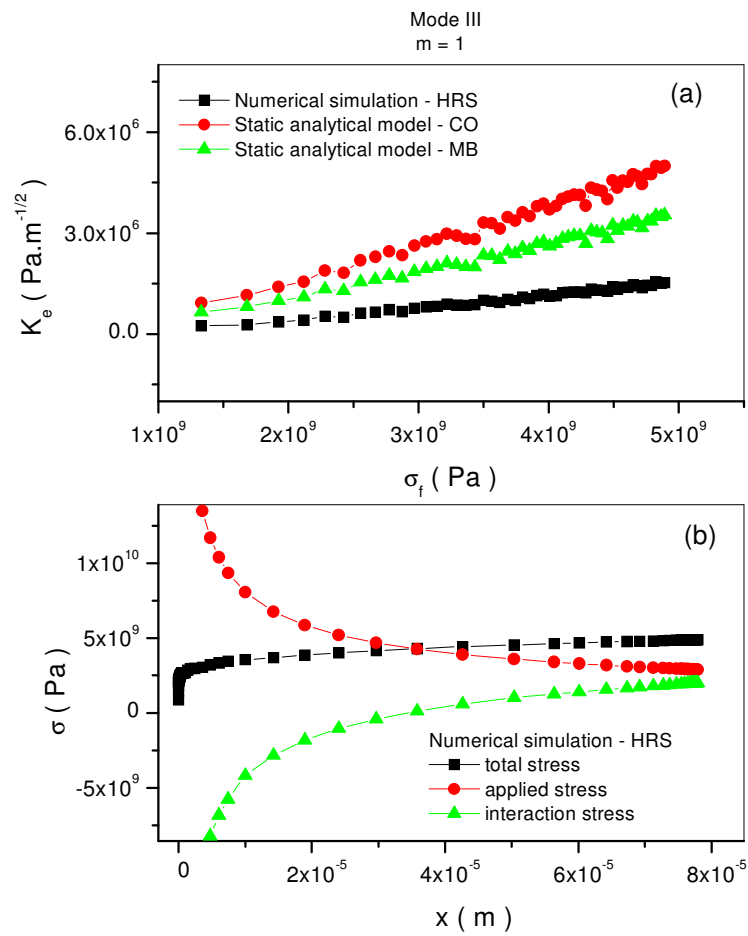


Figure 5. (a) Variation of K_e along the plastic zone as predicted by the models HRS, CO and MB and (b) stress components and total stress according to the HRS model along the plastic zone.

6. Acknowledgements

A. Mikowski is grateful for CAPES for financial support.

7. References

- Booth, A.S., Roberts, S.G., 1997, "The brittle-ductile transition in γ -TiAl single crystals", *Acta materialia*, Vol. 45, pp. 1017-1023.
- Byrd, P. F.; Friedman, M. D., 1954, "Handbook of Elliptic Integrals for Engineers and Physicists", Ed. Springer-Verlag, Berlin, p. 1-281.
- Chang, S. J.; Ohr, S. M., 1981, "Dislocation-free zone model of fracture", *Journal Applied Physics*, Vol. 52, pp. 7174-7181.
- Chen, J., Kitaoka, S., 1999, "Distribution of dislocation at a mode I crack tip and their shielding effect", *International Journal of Fracture*, Vol.100, pp. 307-320.
- Chen, J.; Takezono, S., 1995, "The dislocation-free zone at a mode I crack tip", *Engineering Fracture Mechanics*, Vol. 50, pp. 165-173.
- Gumbsch, P., Riedle, J., Hartmaier, A., Fischmeister, H. F., 1998, "Controlling factors for the brittle-to-ductile transition in tungsten single crystals", *Science*, Vol. 282, pp. 1293-1295.
- Head, A. K.; Louat, N., 1955, "The distribution of dislocations in linear arrays", *Aust. Journal of Physics*, Vol. 8, pp. 1-7.
- Hirsch, P.B., Roberts, S.G., Samuels, J., 1989, "The brittle-ductile transition in silicon. II Interpretation", *Proc. Royal Society London A.*, Vol. 421, pp. 25-53.
- Majumdar, B. S.; Burns, S. J., 1983, "A Griffith crack shielded by a dislocation pile-up", *International Journal of Fracture*, Vol. 21, pp. 229-240.
- Muskhelishvili, N. I., 1953, "Singular Integral Equations", Ed. P. Noordhoff, Groningen, pp. 251-253.
- Roberts, S. G., 1997, "Modelling crack tip plastic zones and brittle-ductile transitions", *Materials Science and Engineering A*, Vol. 234, pp.52-58.
- Serbena, F. C., 1995, "The Brittle-Ductile Transition of NiAl Single Crystals. London", D. Phil. Thesis, University of Oxford, Oxford, UK, 133 f.
- Serbena, F.C., Roberts, S.G., 1994, "The brittle-to-ductile transition in germanium", *Acta metallurgica.*, Vol. 42, pp. 2505-2510.